

## NEW INSIGHTS INTO THE TEMPORAL EVOLUTION OF MBPS

D. UTZ<sup>1,2</sup>, J. C. del TORO INIESTA<sup>2</sup>, L. R. BELLOT RUBIO<sup>2</sup>, J. JURČÁK<sup>3</sup>,  
S. THONHOFER<sup>1</sup>, M. BODNÁROVÁ<sup>4</sup>, A. HANSLMEIER<sup>1</sup>,  
B. LEMMERER<sup>1</sup>, I. PIANTSCHITSCH<sup>1</sup> and S. GUTTENBRUNNER<sup>1</sup>

<sup>1</sup>*IGAM/Institute of Physics, Karl Franzens University of Graz,  
Universitätsplatz 5, AT-8010 Graz, Austria*

<sup>2</sup>*Instituto de Astrofísica de Andalucía (CSIC),  
Apdo. de Correos 3004, E-18080 Granada, Spain*

<sup>3</sup>*Astronomical Institute of the Czech Academy of Sciences,  
Fričova 298, CZ-251 65 Ondřejov, Czech Republic*

<sup>4</sup>*Astronomical Institute of the Slovak Academy of Sciences,  
SK-059 60 Tatranska Lomnica, Slovak Republic*

**Abstract.** Magnetic bright points (MBPs) are among the most fascinating and interesting manifestations of small-scale solar magnetic fields. In the present work the temporal evolution of MBPs is followed in data sets taken by the Hinode satellite. The analysed data and obtained results confirm a recently presented study done with Sunrise/IMaX data, namely that MBPs are features undergoing fast evolution with magnetic fields starting around the equipartition field strength, then showing strong downflows (between 2 to 4 km/s) causing the magnetic field to amplify into the kG range (700 to 1500 G) before dissolving again. Furthermore the initial field inclinations depend on the initial magnetic field strengths and show an evolution with more vertical angles at some point during the evolution.

**Key words:** small-scale solar magnetic fields - spectropolarimetry - Hinode

### 1. Introduction

The magnetic fields of the Sun are responsible for its activity and cause plentiful of interesting phenomena. Among the interesting features on the smallest observable scales are the so-called magnetic bright points (MBPs). First observed in the 70's (e.g., Dunn and Zirker, 1973) they attracted lots of interest in the 80's when the community started to use the G-band filter for identifying them (e.g., Muller, 1983). Nowadays their dynamics (velocities, lifetimes, e.g., Bodnárová *et al.*, 2013) as well as their static parameters

(such as brightness, size, e.g., Wiehr *et al.*, 2004) are studied in full detail. Yet, there are many open questions such as, how is the magnetic field stabilised and when it finally breaks down and the feature dissolves, how is this process evolving and what happens to the energy stored in the magnetic field.

In this proceeding we try to get a more complete understanding of the evolution of MBPs by tracking them in a Hinode data set consisting of filtergram data as well as inversion products created from spectropolarimetric data. Firstly we will have a look on one detailed example before showing statistical interferences from all of the tracked MBPs later on.

## 2. Data

The data were obtained by the solar telescope (SOT; Tsuneta *et al.*, 2008) onboard of the 2006 space-borne satellite Hinode (Kosugi *et al.*, 2007). We use a data set consisting of G-band data taken by the broad-band filter imager (BFI) as well as spectropolarimetric data taken by the SP (spectropolarimeter). All the data sets have been carefully reduced by the corresponding SSW IDL routines. Moreover, the SP data have been inverted with the MERLIN inversion code and the inversion products were then rescaled to the G-band data. Finally, all the data at hand (G-band, intensity map, temperature map, magnetic field strength, LOS velocity map and inclination map) have been co-aligned and cut to the same size (an automated algorithm for these tasks is available and described in full detail in Kuehner *et al.*, 2010). Figure 1 illustrates the data set by showing a small detail of the FOV of all the available data products.

## 3. Analysis

To be able to analyse the evolution of MBPs we have to track them and follow different interesting parameters. For this purpose we applied a fully automated segmentation and identification routine described in Utz *et al.* (2009, 2010) on the G-band data. After the identification of the features in single images we had to combine that information to form complete evolutionary tracks. This is done by adding pointers to the identified MBPs pointing to the previous and following realisation of the MBP (more information about this tracking procedure can be found in Utz *et al.*, 2014).

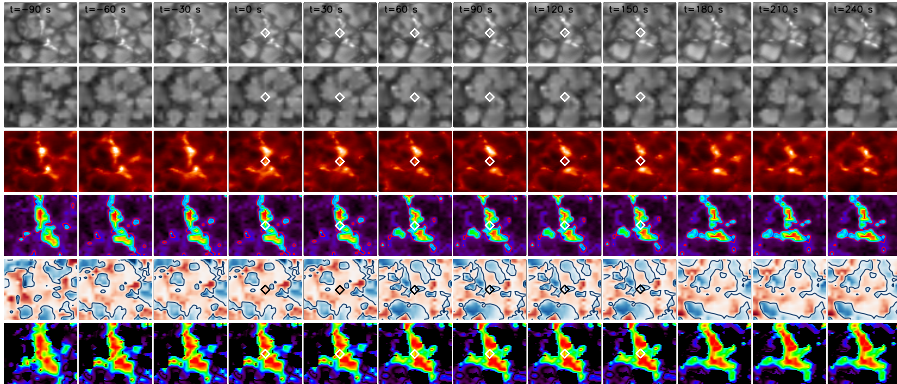


Figure 1: From top to bottom: A detail of the G-band image, intensity map obtained from the spectro-polarimeter, Ca II H map, products from the MERLIN inversions: magnetic field strength map, LOS velocity map and field inclination. The tracked MBP feature is marked by a diamond the time is given in the top row. All the data (SP-data and inverted data) have been scaled to the G-band resolution (BFI).

#### 4. Results

Figure 1 illustrates the tracking of one MBP in several maps of interesting parameters. From top to bottom these are the G-band, the intensity of the spectropolarimetric data, the Ca II H filtergram and products from the Merlin inversion such as magnetic field strength, LOS velocity and inclination. The MBP is clearly visible in the G-band and in the Ca II H data in which it fades away a bit earlier than in the G-band. This MBP is part of a group of MBPs belonging to some extended magnetic field patch as can be seen in the magnetic field strength map and inclination map. The LOS velocity map shows that it is formed in a downflowing intergranular region.

Figure 2 gives the extracted plasma parameters for this particular MBP. A clear response can be seen in the G-band as well as in the chromospheric Ca-II H intensity curves. Furthermore it is visible that the magnetic field existed already before the formation of the MBP (about 1 kG) and does not change too much during the evolution. Finally, when the MBP dissolves, the field drops down to values of a few hundred G (400 G). The LOS velocity shows an increase to 1.5 km/s just before the onset of the bright point which then drops down to lower values and nearly ceases after the formation of

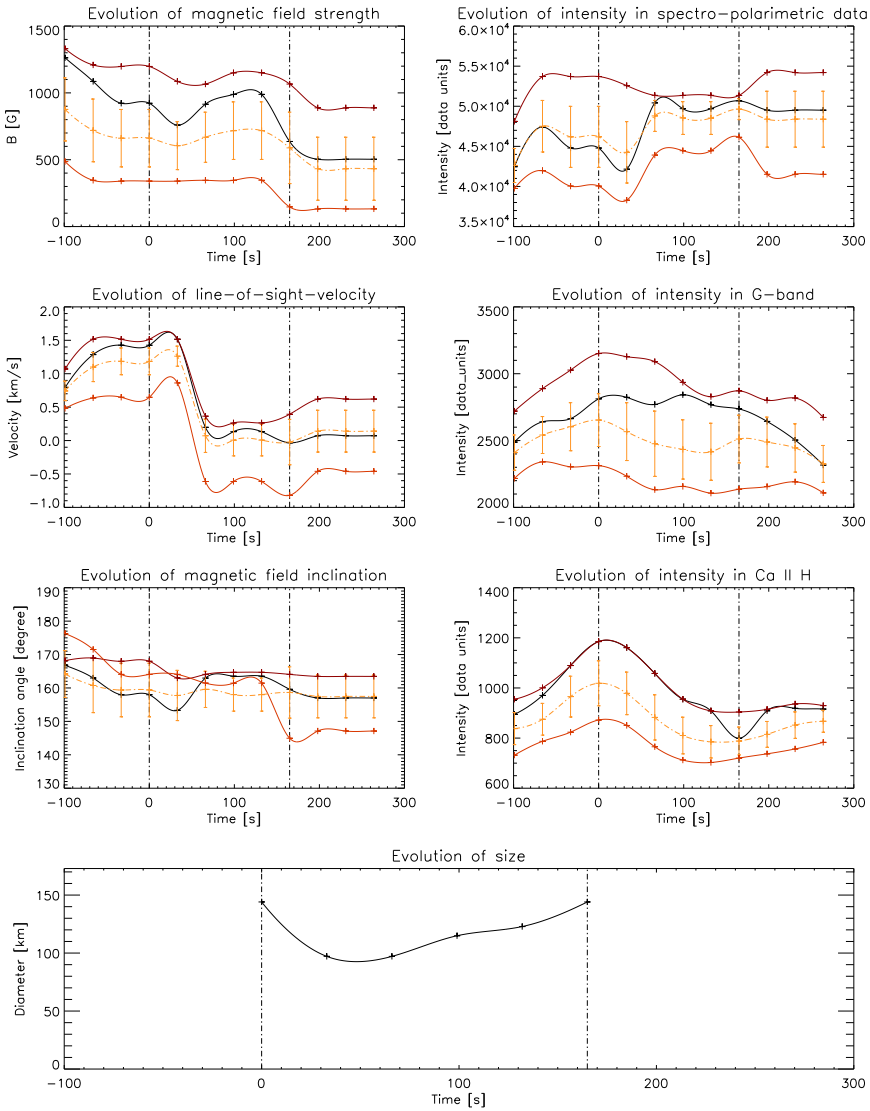


Figure 2: Gives the temporal evolution of the studied plasma parameters of the tracked MBP of Fig. 1. From top to bottom (left column): The magnetic field strength, the LOS velocity, the field inclination, the size of the feature; right column: the intensity in the spectropolarimetric data, the G-band intensity, and the Ca II H intensity; Black lines correspond to barycentre values; dark-red, orange, yellow lines to maxima, minima and averages in a 5 by 5 pixels<sup>2</sup> subfield around the barycentre. The dashed vertical lines mark the starting and ending of the tracking of the feature.

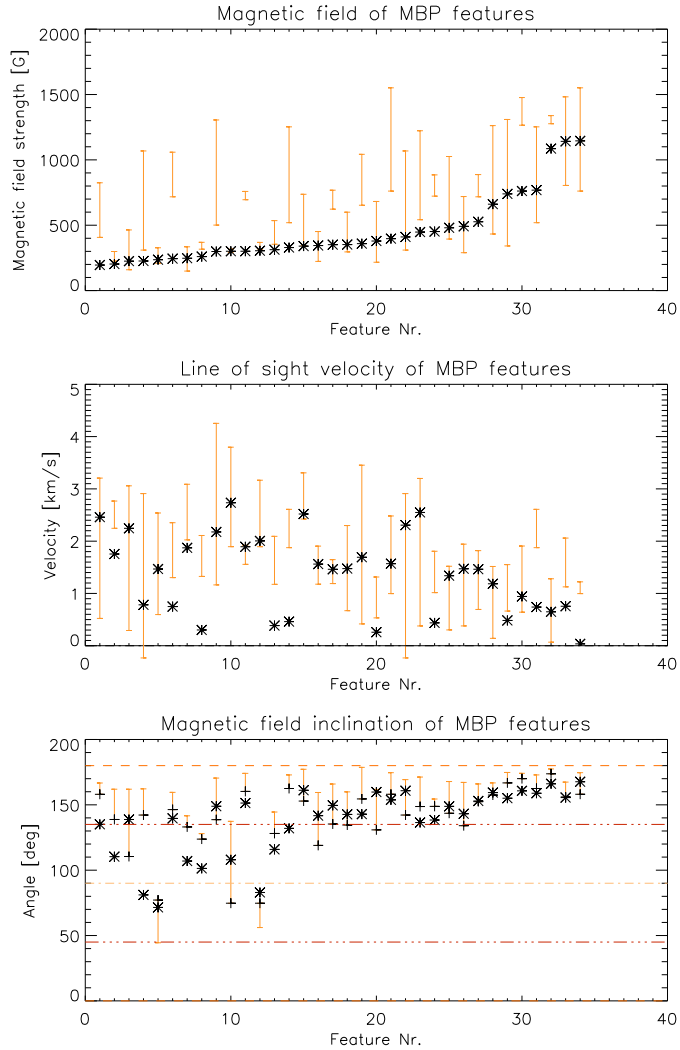


Figure 3: From top to bottom: The magnetic field strength distribution, the LOS velocity distribution, and the magnetic field inclinations of all the tracked MBPs are displayed with increasing initial magnetic field strengths. The vertical bars give the final and maximum value of the quantities, whereas the symbol represents the initial value. The dashed lines, in the case of the inclinations, illustrate the domains of the outwards pointing and inwards pointing magnetic field (the 2 polarities). Besides the 45 and 135 degree lines are plotted to indicate the boundary between vertical and horizontal fields.

the MBP. The size of the feature shows an expected behaviour, namely a shrinkage in the beginning and then a rather slow increase in size when the feature fades away.

The last results we wish to discuss are depicted in Fig. 3. Here we show from top to bottom the magnetic field strength, LOS velocity, and field inclination for all of the tracked MBPs in the used Hinode data set. The magnetic field strengths are sorted from smaller initial magnetic field strengths to larger ones. It is remarkable that this sorting of the magnetic field strengths also lead to a kind of sorting within the other 2 studied parameters. Namely that LOS velocities generally tend to have lower values when the initial magnetic field strength is higher and that the field is more vertically orientated for stronger fields.

### **Acknowledgements**

The research was funded by the Austrian Science Fund (FWF): J3176. In addition D.U. wish to thank the Österreichischer Austauschdienst (ÖAD) and the Ministry of Education Youth and Sports (MŠMT) of the Czech Republic for financing a short research stay at the Astronomical Institute of the Czech Academy of Sciences in Ondřejov in the frame of the project MEB061109. Furthermore, J.J. wants to express vice versa his gratitude to the MŠMT and ÖAD for financing a short research stay at the IGAM of the University of Graz. Moreover, J.J. is grateful for support from the Czech Science Foundation (GACR) through project P209/12/0287 and RVO:67985815. Partial funding has also been obtained from the Spanish Ministerio de Economía through Projects AYA2011-29833-C06 and AYA2012-39636-C06, including a percentage of European FEDER funds. Hinode is a Japanese mission developed and launched by ISAS/JAXA, collaborating with NAOJ as a domestic partner, NASA and STFC (UK) as international partners. Scientific operation of the Hinode mission is conducted by the Hinode science team organized at ISAS/JAXA. This team mainly consists of scientists from institutes in the partner countries. Support for the post-launch operation is provided by JAXA and NAOJ (Japan), STFC (U.K.), NASA (U.S.A.), ESA, and NSC (Norway). Hinode SOT/SP Inversions were conducted at NCAR under the framework of the Community Spectro-polarimetric Analysis Center (CSAC; <http://www.csac.hao.ucar.edu/>)

## References

- Bodnárová, M., Utz, D., and Rybák, J.: 2013, *Solar Phys.* **289**, 1543.
- Dunn, R. B. and Zirker, J. B.: 1973, *Solar Phys.* **33**, 281.
- Kosugi, T., Matsuzaki, K., Sakao, T., Shimizu, T., Sone, Y., Tachikawa, S., Hashimoto, T., Minesugi, K., Ohnishi, A., Yamada, T., Tsuneta, S., Hara, H., Ichimoto, K., Suematsu, Y., Shimojo, M., Watanabe, T., Shimada, S., Davis, J. M., Hill, L. D., Owens, J. K., Title, A. M., Culhane, J. L., Harra, L. K., Doschek, G. A., and Golub, L.: 2007, *Solar Phys.* **243**, 3.
- Kuehner, O., Utz, D., Hanslmeier, A., Veronig, A., Roudier, T., Muller, R., and Muthsam, H.: 2010, *Cent. Eur. Astrophys. Bull.* **34**, 31.
- Muller, R.: 1983, *Solar Phys.* **85**, 113.
- Tsuneta, S., Ichimoto, K., Katsukawa, Y., Nagata, S., Otsubo, M., Shimizu, T., Suematsu, Y., Nakagiri, M., Noguchi, M., Tarbell, T., Title, A., Shine, R., Rosenberg, W., Hoffmann, C., Jurcevich, B., Kushner, G., Levay, M., Lites, B., Elmore, D., Matsushita, T., Kawaguchi, N., Saito, H., Mikami, I., Hill, L. D., and Owens, J. K.: 2008, *Solar Phys.* **249**, 167.
- Utz, D., del Toro Iniesta, J. C., Bellot Rubio, L. R., Jurčák, J., Martínez Pillet, V., Solanki, S. K., and Schmidt, W.: 2014, *Astrophys. J.* p. submitted.
- Utz, D., Hanslmeier, A., Möstl, C., Muller, R., Veronig, A., and Muthsam, H.: 2009, *Astron. Astrophys.* **498**, 289.
- Utz, D., Hanslmeier, A., Muller, R., Veronig, A., Rybák, J., and Muthsam, H.: 2010, *Astron. Astrophys.* **511**, A39.
- Wiehr, E., Bovelet, B., and Hirzberger, J.: 2004, *Astron. Astrophys.* **422**, L63.